

ARTICLE

Open Access

A metasurface-based light-to-microwave transmitter for hybrid wireless communications

Xin Ge Zhang¹, Ya Lun Sun¹, Bingcheng Zhu^{2,3,4}, Wei Xiang Jiang^{1,3,4}, Qian Yu¹, Han Wei Tian¹, Cheng-Wei Qiu⁵, Zaichen Zhang^{2,3,4} and Tie Jun Cui¹

Abstract

Signal conversion plays an important role in many applications such as communication, sensing, and imaging. Realizing signal conversion between optical and microwave frequencies is a crucial step to construct hybrid communication systems that combine both optical and microwave wireless technologies to achieve better features, which are highly desirable in the future wireless communications. However, such a signal conversion process typically requires a complicated relay to perform multiple operations, which will consume additional hardware/time/energy resources. Here, we report a light-to-microwave transmitter based on the time-varying and programmable metasurface integrated with a high-speed photoelectric detection circuit into a hybrid. Such a transmitter can convert a light intensity signal to two microwave binary frequency shift keying signals by using the dispersion characteristics of the metasurface to implement the frequency division multiplexing. To illustrate the metasurface-based transmitter, a hybrid wireless communication system that allows dual-channel data transmissions in a light-to-microwave link is demonstrated, and the experimental results show that two different videos can be transmitted and received simultaneously and independently. Our metasurface-enabled signal conversion solution may enrich the functionalities of metasurfaces, and could also stimulate new information-oriented applications.

Introduction

Signal conversion between optical and radio frequency (RF) domains is the basis and key to realize hybrid systems employing both optical and RF communication technologies^{1–5}. The hybrid optical and RF communication systems can release the limitations of the individual systems and provide positive features of them, which is identified as a promising way to support multi-domain integrated and full-spectrum networks for future sixth generation (6G) wireless communications^{6–10}. So far, the mixed communications are realized typically through the cooperative relaying systems where the received optical signals

(or RF signals) are firstly amplified and converted to baseband before being down-converted to the RF (or up-converted to optical) domains. This solution needs a large number of optical components, RF devices, and multiple process steps that eventually make the hybrid systems with high cost and high complexity. Recently, plasmonic-enabled schemes for direct conversions of millimeter and terahertz waves to the optical signals have been implemented, which lead to a significant leap forward toward the low-complexity and cost-efficiency wireless-to-fiber communication systems^{2,3}. In contrast to that, the device that can encode directly a light signal onto a microwave carrier for the optical-to-RF hybrid wireless communication has not yet been demonstrated.

Metasurfaces are two-dimensional (2D) artificial structures with precisely engineered elements in sub-wavelength scales, which have unfolded many remarkable approaches to manipulate the electromagnetic (EM) waves and overcome several metamaterial challenges of

Correspondence: Wei Xiang Jiang (wxiang81@seu.edu.cn) or

Zaichen Zhang (zczhang@seu.edu.cn) or Tie Jun Cui (tjcui@seu.edu.cn)

¹State Key Laboratory of Millimeter Waves, School of Information Science and Engineering, Southeast University, 210096 Nanjing, China

²National Mobile Communications Research Laboratory, School of Information Science and Engineering, Southeast University, 210096 Nanjing, China

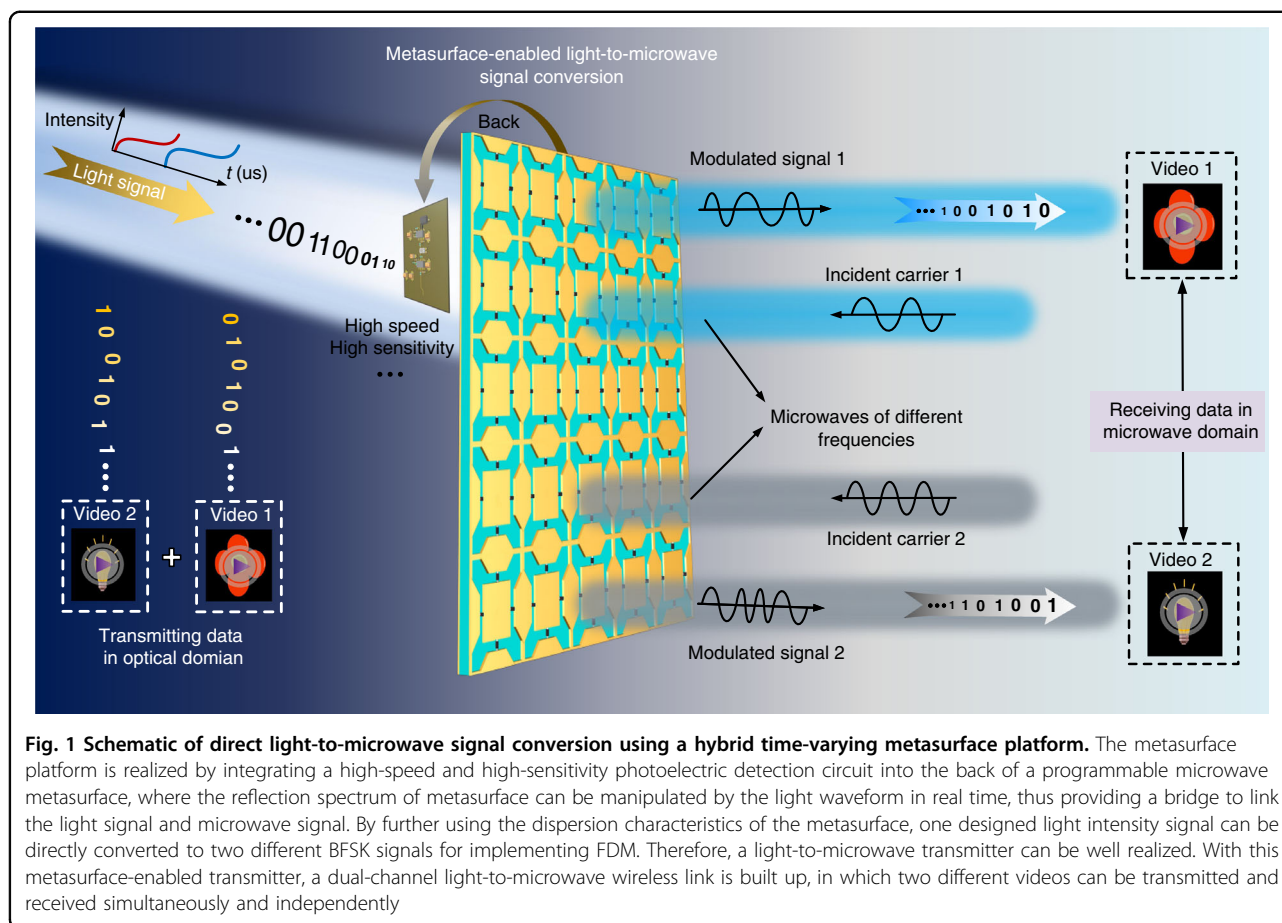
Full list of author information is available at the end of the article

These authors contributed equally: Xin Ge Zhang, Ya Lun Sun, Bingcheng Zhu

© The Author(s) 2022



Open Access This article is licensed under a Creative Commons Attribution 4.0 International License, which permits use, sharing, adaptation, distribution and reproduction in any medium or format, as long as you give appropriate credit to the original author(s) and the source, provide a link to the Creative Commons license, and indicate if changes were made. The images or other third party material in this article are included in the article's Creative Commons license, unless indicated otherwise in a credit line to the material. If material is not included in the article's Creative Commons license and your intended use is not permitted by statutory regulation or exceeds the permitted use, you will need to obtain permission directly from the copyright holder. To view a copy of this license, visit <http://creativecommons.org/licenses/by/4.0/>.



bulky, lossy and fabrication, enabling a broad range of applications^{11–26}. As an emerging technology, programmable metasurfaces allow real-time EM manipulations and information processing, which have shown great potentials to construct RF-chain-free transmitters and new paradigms of 6G intelligent and programmable wireless environment^{27–33}. However, the mostly used electrical control method to date limits the programmable metasurfaces to be only considered in a single domain and thus blocks their transition to advanced optoelectronic hybrid multi-physics platforms that can process the optical and RF signals simultaneously. We have previously reported the photodiode-based light-controllable microwave metasurfaces^{13–15}, on which the EM functions can be programmed by visible light, but the scheme of just loading the photodiode array onto the metasurface is hard to use for wireless communication due to the slow switching speed.

In this article, we report a hybrid metasurface-based transmitter for direct signal conversion from visible lights to microwaves. Such the hybrid transmitter is implemented by an optically programmed time-varying metasurface, which is constructed via the heterogeneous integration of a high-speed and linear photoelectric

detection circuit into a reflective programmable metasurface. The profile of the whole platform is around 0.04λ at 6.0 GHz. When receiving a modulated light signal, the metasurface platform is able to convert the light signal to the microwave domain directly without using down-conversion process to baseband. More importantly, one designed light signal can carry two independent original information that can be encoded onto two microwave carriers with different incidence frequencies by using the dispersion characteristic of the metasurface. Based on the light-to-microwave metasurface transmitter, we realize a dual-channel hybrid wireless communication system that can transmit simultaneously two different videos with the aid of frequency division multiplexing (FDM) scheme.

Results

Encoding a light signal onto two microwave carriers via metasurface

Figure 1 presents the scheme for the direct conversion of a light signal to microwave signals by just using a single planar hybrid time-varying metasurface platform, without any additional RF devices and optical components. The metasurface platform consists of a varactor-based dynamic wideband metasurface and a photoelectric detection

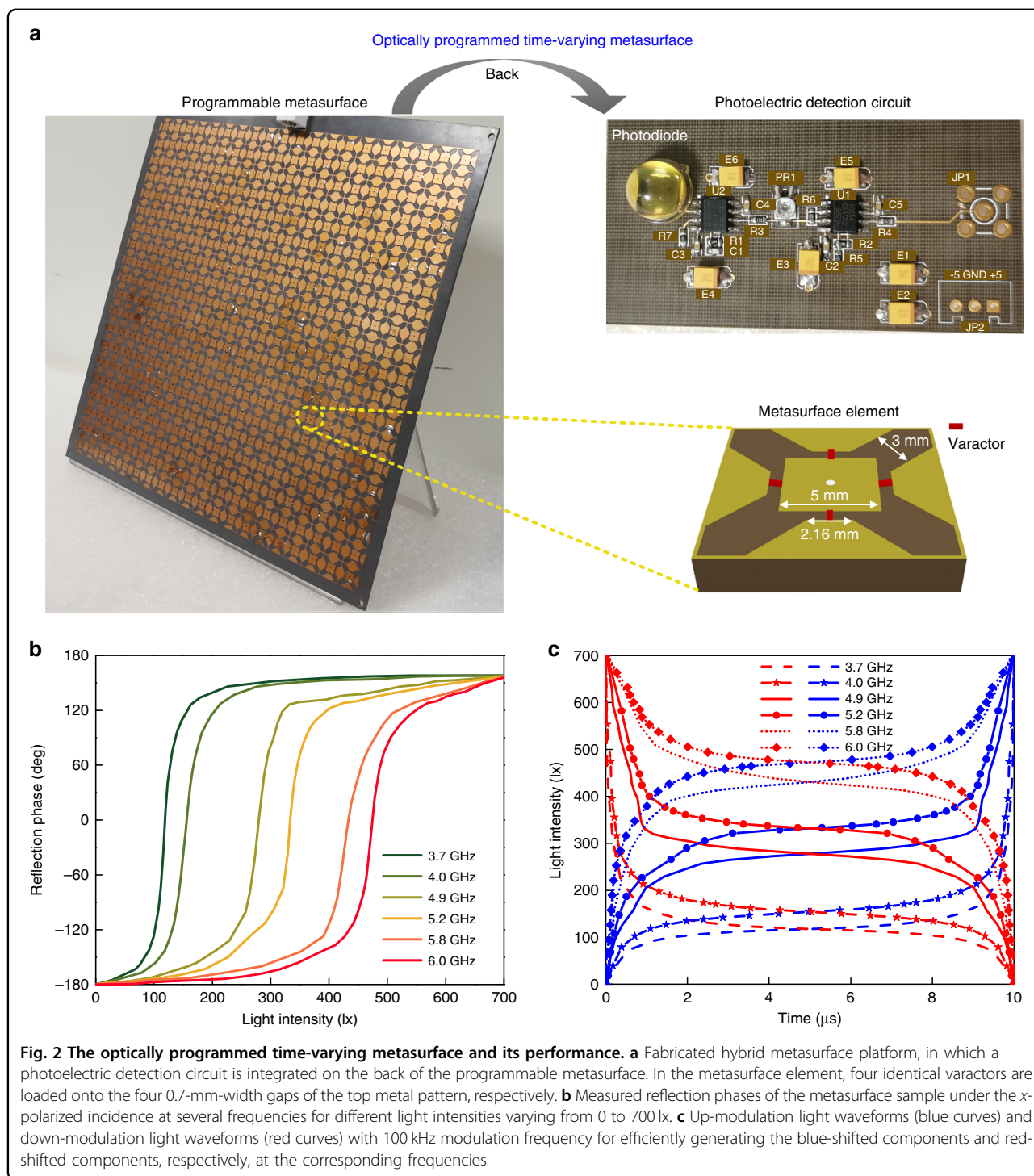
circuit that is composed of a photodiode and two cascaded transimpedance amplifying circuits. With this hybrid integration strategy, the reflection phase of the metasurface can be modulated by light intensity at high speed. When the intensity of the illumination light changes periodically and rapidly in a special waveform, the metasurface will generate a certain reflected harmonic distribution based on the phase modulation under microwave incidence. Therefore, the digital information can be modulated on the waveforms of the light signal and then are mapped directly onto the spectral characteristics of the reflected microwaves, thus achieving the direct light-to-microwave signal conversion and transmission. In this case, the optically programmed time-varying metasurface can be used to construct the light-to-microwave transmitter. Moreover, we explore to use strong dispersion response of the designed metasurface to convert one light signal containing four different sets of modulated waveforms to two different binary frequency shift keying (BFSK) microwave signals. Therefore, two data (e.g., two different videos) can be converted and transmitted through the same metasurface aperture independently and simultaneously for implementing FDM, which improves greatly the information processing capability and efficiency of the metasurface platform.

To support the high bandwidth demand of wireless communications, the optical spectrum is considered as a promising complementary resource of RF, due to the good features of vast license-free spectrum, high security, high energy efficiency, and EM interference free. Compared to the widely used wireless transmission in microwave bands, the visible light communication (VLC) based on light waves is very suitable for many special application scenarios, such as the indoor communication, underwater communication, and data transfer in some EM sensitive environments including hospitals, gas stations, and underground mines. Because the microwave communication and VLC have complementary advantages in communication environments, seamless integration of VLC links into the existing RF wireless infrastructures is of crucial importance for full-spectrum wireless networks. We know that the VLC is a promising method for underwater communication due to relative long-distance communication and high speed, but it is easy to be blocked and disturbed in free space; conversely, microwave communication is widely used in free space, however, microwave has great loss under water and it is not conducive to long-distance transmission⁷. To overcome this limitation, the hybrid transmitter that allows light-to-microwave signal conversion and transmission is very necessary. For example, the light-to-microwave transmitter can be used to receive the modulated light signals from the underwater communication devices, and then transmit these data to the corresponding air receivers

through the microwave link. Our proposed metasurface-enabled direct light-to-microwave signal conversion offers a practical and low-overhead solution to establish such a hybrid transmitter, where the complicated and distributed relay systems are no longer required. In addition, dual-channel data transmissions are achieved based on FDM for improving the capacity of the hybrid wireless network.

Time-varying metasurfaces with dynamic harmonic control capability have been demonstrated as an effective information delivery mechanism^{34–38}. Different from the electrically controlled time-modulated metasurfaces, we design and fabricate an optically programmed time-varying metasurface (Fig. 2a), in which the reflection spectrum of metasurface can be controlled by visible light. Key to the multi-physics field platform is to integrate fully a microsecond level optoelectronic circuit into a microwave metasurface. The front of the hybrid metasurface sample is the arranged periodically dynamic metasurface elements, each of which has a 90° rotationally symmetric metal pattern printed on a polytetrafluoroethylene glass cloth copper clad laminate (F4B) substrate with a dielectric constant of 2.65 and a loss tangent of 0.001. Four identical varactors are symmetrically embedded onto the metal structure for realizing polarization-insensitive and broadband features. Since the resonant frequency of the element is related to the capacitance value, the element bandwidth mainly depends on the capacitance variation range of the used varactor. Here, we adopt the “MAVR-000120-14110P” varactor with a high capacitance ratio of 8.2 (varying from 1.15 to 0.14 pF) to realize the wideband tunability. The back of the metasurface sample is a photoelectric detection circuit, in which the cascaded amplifying circuits are designed to enable the photoelectric detection circuit to generate a large voltage variation range linearly and rapidly. Compared with the series photodiode array in our previous work¹³, the switching frequency of the photoelectric detection circuit is about 10000 times higher and can reach 2 MHz. In such a case, when receiving the visible light with different intensities, the photoelectric detection circuit will convert them to the corresponding voltages for tuning the loaded varactors, and then changes the reflection phase of the incident microwaves in real time. See “Materials and Methods” for more details on circuit principle as well as sample design and fabrication.

Spectrum manipulation depends on the accurate temporal control of the reflection phase. Thus, we firstly test the reflection phases of the metasurface sample at several frequencies for different light intensities, and the measured results are plotted in Fig. 2b. It is clear that when the illumination intensity increases gradually from 0 to ~700 lx, the reflection phase will change accordingly from -180° to around 160°, offering about 340° phase excursions at all test frequencies. We have proved that when



the reflection phase changes linearly in one time period $T = 1/f_v$, the time-varying metasurface will generate a frequency shift f_t upon reflection³⁹. We here use the visible light to drive the metasurface for achieving the high-efficiency frequency manipulation. The required up- and down-modulation optical waveforms are derived from the measured reflection phase curves, which allow

the reflection phase to change linearly with time (Fig. 2c). Controlled by these up- and down-modulation waveforms, the metasurface sample can produce effectively blue- and red-shifts, respectively, corresponding to the frequency shift keying (FSK) in digital modulation formats (see Supplementary Note 1 for more details). Hence, a light waveform signal can modulate directly the reflection

frequency of the metasurface, indicating that the hybrid metasurface platform provides an interface to link the light signal with the microwave FSK signal in real time.

The measured phase curves show a strong dispersion response of the metasurface, as discussed in Supplementary Note 2. Due to the strong dispersion, the required modulation waveforms for efficient frequency conversion at different operating frequencies are obviously different, as shown in Fig. 2c. See Supplementary Note 3 for details on the characteristic of light waveforms. Because the frequency conversion efficiency of the time-varying metasurface highly relies on the control waveform, for a fixed light waveform, the main reflection component can be at the harmonic (good conversion effect) or the fundamental frequency (poor conversion effect) under two microwave incidences with different frequencies. In this case, by employing the fundamental frequency and the frequency-shifted harmonic as two discrete frequencies to implement the BFSK modulation, one light waveform can represent two different digital symbols at these two incident frequencies. To achieve two BFSK signals simultaneously, the bandwidth selection of the two incident frequencies is crucial for implementing FDM. More details are provided in “Materials and methods”. As demonstrations, we adopt 5.2 and 4.9 GHz microwaves as the two single tone incident subcarriers. Without losing generality, we use the fundamental frequency and the blue-shifted frequency to represent the digital symbols ‘0’ and ‘1’, respectively.

The designed four light waveforms and the correspondingly measured spectral distributions of the metasurface at 5.2 and 4.9 GHz are plotted in Fig. 3, which illustrate the dual-channel signal conversion process. Two independent data streams are encoded onto the four sets of different light waveforms. The light waveform W_1 is a direct-current control waveform (Fig. 3a), in which the light intensity is not changed with time and thus the frequencies of both reflected BFSK signals are at the original fundamental frequencies of 5.2 and 4.9 GHz (Fig. 3e). In this case, two digital symbols ‘0’ are transferred successfully from the light signal to the microwave domain. The light waveforms W_2 and W_3 are the up-modulation waveforms corresponding to 5.2 and 4.9 GHz, respectively (Fig. 3b, c). For light waveform W_2 , the main frequency component of BFSK signal 1 is at the blue-shifted frequency of 5.2001 GHz (related to bit ‘1’), but that of BFSK signal 2 is still at the fundamental frequency of 4.9 GHz (related to bit ‘0’) (Fig. 3f). Similarly, the light waveform W_3 is used to encode the digital symbol ‘0’ onto BFSK signal 1 and digital symbol ‘1’ onto BFSK signal 2, as shown in Fig. 3g. The light waveform W_4 in Fig. 3d is designed to encode the digital symbol ‘1’ onto two BFSK signals simultaneously, where the main frequency components are both blue-shifted frequencies (Fig. 3h).

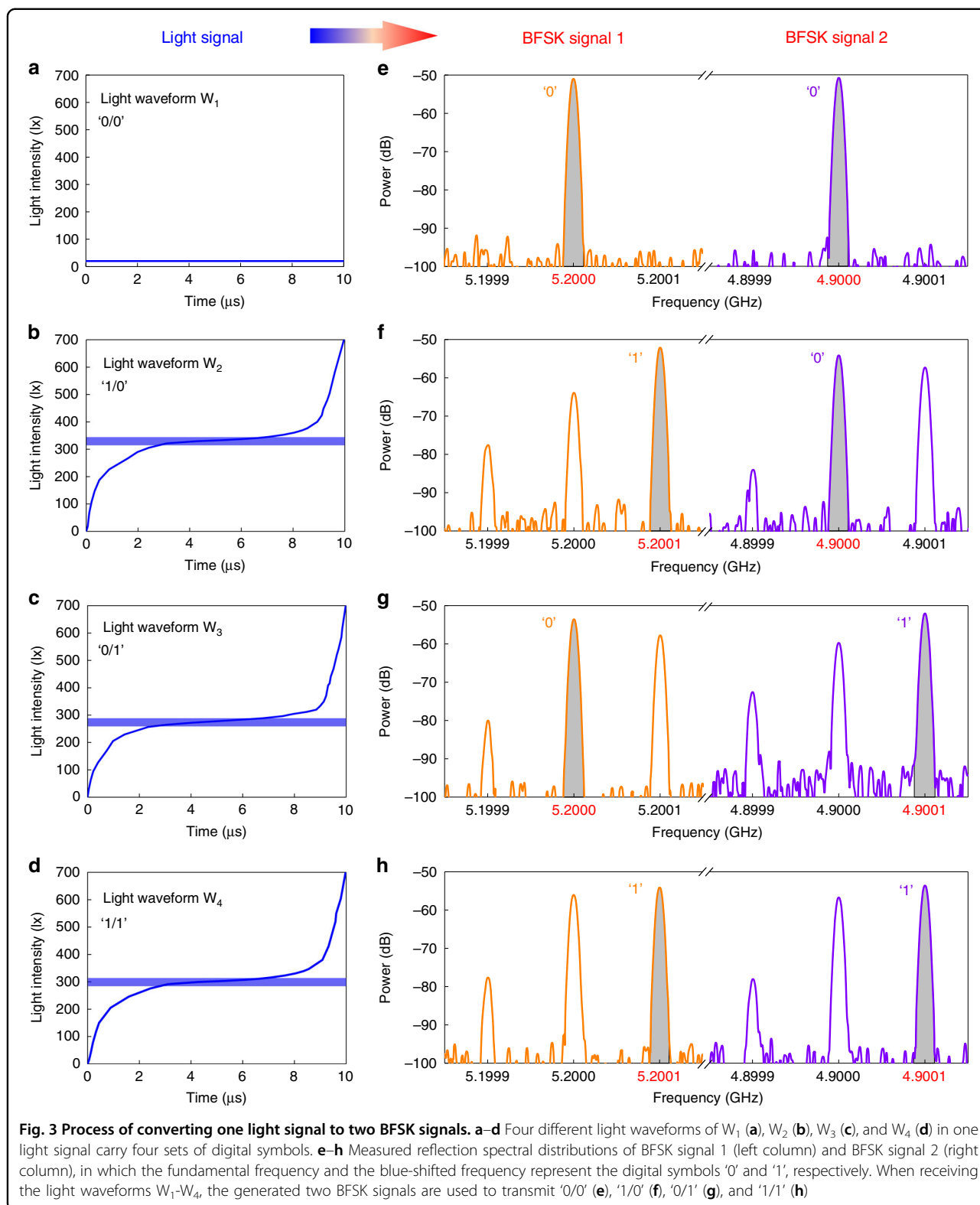
Hence, one light signal that contains the four sets of waveforms can be converted directly to two BFSK signals based on FDM. In this case, the hybrid light-to-microwave transmitter can be well realized by using the optically programmed time-varying metasurface.

Implementation of a dual-channel hybrid communication system

To further verify the proposed scheme of direct light-to-microwave signal conversion and show its potential applications, we build a dual-channel hybrid wireless communication system based on the hybrid metasurface transmitter, as shown in Fig. 4a. The demonstrated hybrid communication system mainly consists of three parts: an optical transmitter, a metasurface signal converter, and a microwave receiver. The optical transmitter contains a light modulation and driving module and a light-emitting diode (LED) light source, which is designed to generate the light signals with the modulated information. In the optical domain, the metasurface-enabled light-to-microwave signal converter acts as an optical receiver for capturing the encoded light signals, while it works as a RF transmitter in the microwave communication link. Two horn antennas in the transmitter are used to provide two incident carriers with different frequencies simultaneously. The microwave receiver mainly contains two receiving horn antennas and a software-defined radio (SDR) platform (NI USRP-2954) connected to a post-processing computer. We remark that the hybrid communication system can implement a light-to-microwave wireless link where complicated relay systems are no longer required. See “Materials and methods” for more details on the system prototype.

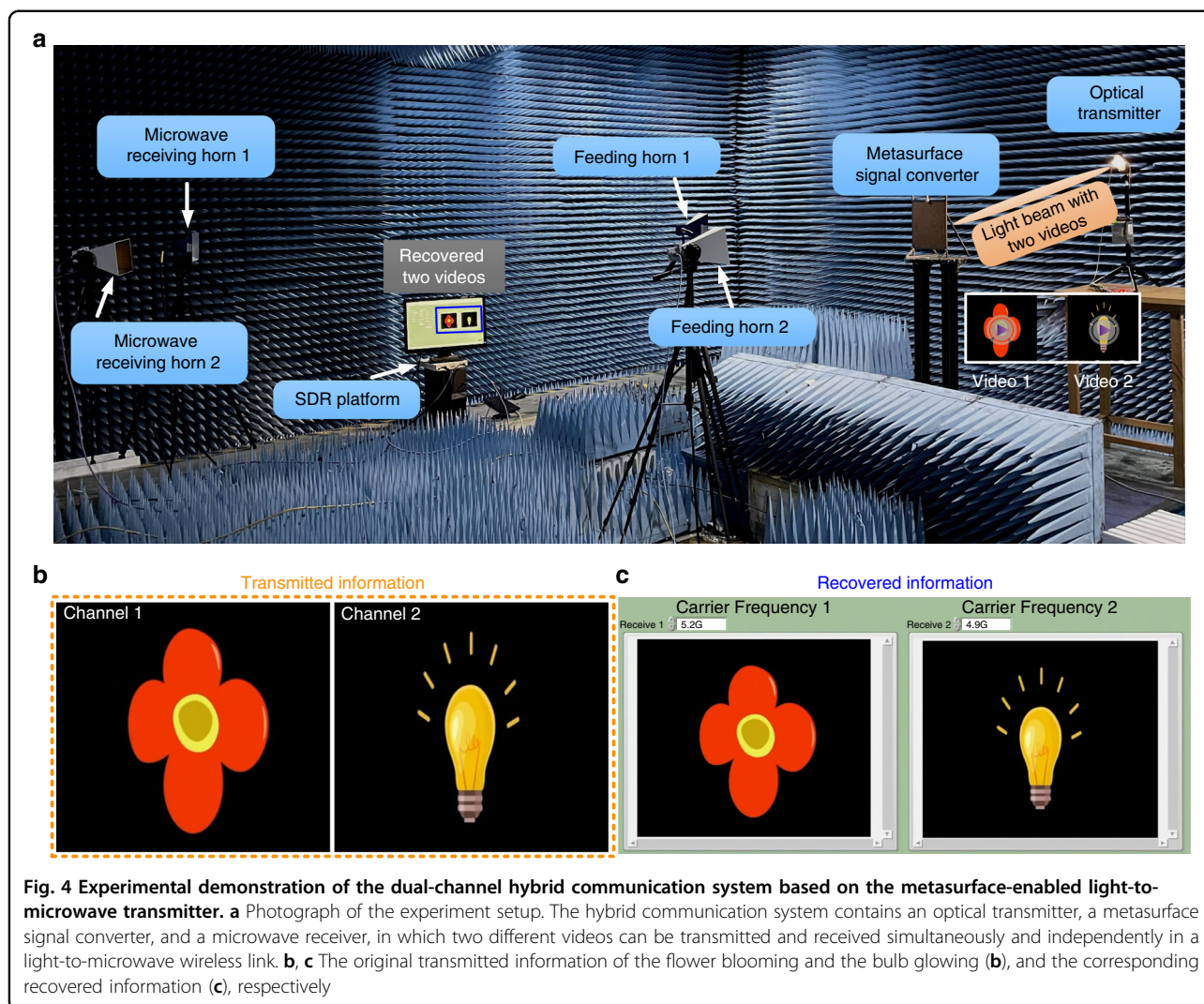
It is important to note that unlike the traditional wireless transmitters, the metasurface-based transmitter is able to modulate directly the baseband signal onto the air-fed carrier waves. In this case, the real-time programmable capability is very critical. For the traditional RF emission sources, such as horn antennas and microstrip antennas, the programmability is hard to achieve, especially for multi-element array. As a typical reconfigurable technology, the phased array antenna has been proposed and realized to control EM waves dynamically. However, the conventional phased array antennas are expensive, and their complex feeding structures and transmitter/receiver modules will affect the performance of antennas. Compared with the phased array antennas, the programmable metasurfaces usually have advantages of simple design and low cost. Moreover, the programmable metasurface can be designed elaborately for achieving the wideband feature to realize the FDM.

To show the communication capability of our constructed light-to-microwave hybrid wireless system, as an example, we demonstrate a real-time dual-channel video



transmission based on the system. In experiments, two different videos (one is the flower blooming and the other is the bulb glowing, Fig. 4b) were firstly converted into

two sets of bit streams that are then encoded onto the light signals with four sets of waveforms W_1 – W_4 through the optical transmitter. Two subcarriers at the frequencies



of 5.2 and 4.9 GHz are emitted from the feeding horn antenna 1 and horn antenna 2, respectively, for exciting the metasurface simultaneously. The light signal with two modulation information (videos 1 and 2) are converted directly to BFSK signals 1 and 2, respectively, by using the above-discussed signal conversion process. These two reflected BFSK signals are then received individually by the two horns and demodulated into the digital baseband signals via the SDR receiver to recover the two videos independently and simultaneously, as shown in Fig. 4c (see “Materials and methods” for detailed workflow of the system prototype). The entire transmission process is given in Supplementary Movie 1 and is described briefly in Supplementary Note 4. The transmission rate of the hybrid communication system is 100 kbps. The results validate that the two videos can be transmitted successfully from the optical transmitting terminal to the microwave receiving terminal by the metasurface-enabled light-to-microwave transmitter.

Discussion

It should be noted that by designing the higher frequency metasurfaces, the proposed hybrid integration strategy could be extended to achieve other types of signal conversion platforms, such as the light-to-terahertz transmitter. Recently, several remarkable tunable components, such as complementary metal-oxide-semiconductor (CMOS)-based chip tile⁴⁰ and microelectromechanical systems (MEMS)⁴¹ have been demonstrated for realizing programmable terahertz metasurfaces. By combining these programmable terahertz metasurfaces with appropriate design of photoelectric detection circuit, it is possible to extend our concept of hybrid communication system to higher frequencies, which will help to develop more multi-physics metasurfaces, significantly expanding the potential applications of the metasurfaces. In fact, except for communication application, metasurfaces have also shown many other interesting functions, such as multichannel 3D meta-holography⁴², off-axis multi-color imaging⁴³,

dynamic full-color digital holographic display⁴⁴ and metasurface-based quantum photonics⁴⁵.

Although the proposed joint control scheme of the photodiode-based circuit and varactor is very effective and robust^{13–15,46}, it will add an additional photoelectric conversion step. To achieve the all-optical tuning, one promising solution is to integrate photodiode or photosensitive material such as silicon^{47,48} into the metasurface element directly. In this case, the EM response of metasurface can be controlled by changing the characteristics of photosensitive components with light illumination, without involving any electrosensitive diodes.

In summary, we have demonstrated a metasurface-based transmitter that enables direct signal conversion from the visible light to microwaves for VLC/RF hybrid communication applications. The low-profile hybrid metasurface platform is realized by integrating a photoelectric detection circuit into a time-varying microwave metasurface. The experimental results verified that the reflection frequency of the metasurface platform can be controlled by the light intensity waveform in real time, thus achieving the FSK modulation. We have also presented an actual scheme of simultaneously converting one light signal to two BFSK signals by utilizing the dispersion characteristics of the metasurface. To demonstrate our approach, we constructed and tested a dual-channel hybrid wireless communication system, in which two different videos can be transferred from the optical transmitter to microwave receiving terminal simultaneously and independently based on the FDM technology. Because the light-to-microwave signal conversion process can be completed fully on a single platform, our metasurface-enabled transmitter shows extraordinary potentials to implement low-cost and low-complexity hybrid communication systems, which are fundamentally important to multi-domain integrated 6G wireless communications^{49,50}.

Materials and methods

Working principle of the photoelectric detection circuit

The simplified diagram of the designed photoelectric detection circuit is presented in Fig. S1. Under light illumination, the photodiode will produce a weak photocurrent I_{pd} , which can be converted into voltage by the transimpedance amplifying circuit and the output voltage is $U_2 = I_{pd} \times R_1$. Then, the voltage U_2 will be further amplified by the post amplifying circuit, and the final generated driving voltage is $U_1 = -U_2 \times R_2/R_3$. In this case, the maximum output voltage of the photoelectric detection circuit can be controlled by tuning the resistance values. Moreover, except for the amplification capability, the cascaded amplifying circuit also provides a low-resistance current loop for the photodiode. Therefore, the photodiode is able to complete the charge-discharge process quickly, resulting in a high switching

speed. As a comparison, we have measured the response speeds of the designed photoelectric detection circuit and the series photodiode array in our previous work¹³. In experiments, we use the time-varying light with the periodic square wave frequency to illuminate these two different photodiode circuits, and the measured output voltage waveforms are shown in Fig. S2a, b, respectively. It is obvious that the switching frequency of the photoelectric detection circuit is able to reach 2 MHz, but that of the photodiode array is only about 200 Hz. The reason is that the previous photodiode array has no current loop and thus the charges are difficult to release from the photodiodes, which can also be seen from the falling edge of its output square wave.

Sample design and fabrication

The size of metasurface element is 12 mm × 12 mm and the height of the grounded F4B dielectric is optimally set as 2 mm. The other geometric parameters of the element are shown in Fig. 2a. The metasurface element is identical to that in our previous work³⁹, but is controlled by light here. To achieve a high reflectivity and a large phase difference, the frequency range of the element is preferably 4.0 to 6.3 GHz. More details on the analysis and results of the element can be found in ref. ³⁹. The pre-amplifier connected to the “S6968” photodiode is a low-noise “OPA657U” amplifier, which allows the generated weak photocurrent to be detected accurately. The post-amplifier connected to the metasurface is an “AD8065ARZ” amplifier with strong driving capability. With this configuration, the high-speed photoelectric detection circuit is linear and can generate a maximum voltage of ~10 V under light illumination. The fabricated sample contains 20 × 20 elements and all the elements are driven uniformly by the connected photoelectric detection circuit. Because the bare dielectric area around the metasurface elements is without a metal ground and this area is very small compared with the periodic element array, it has almost no effect on the reflection performance of the metasurface. The measured reflection efficiencies of the metasurface sample at two working frequencies are 67.2% and 66.4%, respectively. The loss of the metasurface mainly comes from the equivalent resistance of the used varactors. To improve the energy efficiency, we can select carefully the varactor with a smaller equivalent resistance. Recently, a beneficial strategy has been proposed to design and realize the self-filtering metasurface with pure modulated wave²⁴, which is able to improve the transfer efficiency by 83% compared with the traditional approach.

Frequency interval of two subcarriers in FDM

The measured spectral distributions of the time-varying metasurface (Fig. S3a–c) show that the reflected frequency

can be controlled by light signal in real time. The two symmetrically distributed blue-shifted and red-shifted components can be used naturally to provide a pair of discrete frequencies in BFSK. But in this manner, one light signal can only be converted to one BFSK signal. To generate two BFSK signals, the two incident subcarriers should be selected first. We remark that the bandwidth of the subcarriers is very important. If the bandwidth is too narrow, a light waveform will generate the similar frequency modulation effect at the two frequencies and thus it cannot represent two different digital information simultaneously. If the frequency interval is too large, it is difficult to design a light waveform to produce high-efficiency blue shifts at both frequencies. According to multiple measurement results, we find that the dual-channel signal conversion can be realized via the FDM scheme when the bandwidth of two subcarriers is ~ 300 MHz.

Details on system prototype

The hybrid communication system was built in a microwave chamber. The light modulation and driving module were implemented by an FPGA and a digital-to-analog converter (DAC). To generate the required light waveform accurately, a linear focusing LED light source was designed and fabricated. In the experiments, the distance from the light source to the back of the metasurface sample was 2.0 m. In this case, the generated light beam with modulation waveforms can be well focused onto the photoelectric detection circuit. The feeding horn antennas 1 and 2 were connected to an Agilent N5230C vector network analyzer and a Keysight E8267D signal generator to emit the monochromatic waves with frequencies of 5.2 and 4.9 GHz, respectively. The height of the horn antenna 1 is 136 mm, and the length and width of the horn aperture are 150 and 114 mm, respectively. The corresponding physical dimensions of the horn antenna 2 are 260, 170 and 120 mm, respectively. Both feeding horns are 2.4 m away from the front of the metasurface sample. Because the metasurface requires the primary feed antenna, it will increase the volume of the whole communication system. To overcome this limitation, one promising solution is to develop the direct radiation-type metasurfaces. Recently, two low-profile radiation-type metasurfaces have been verified experimentally for controlling EM waves flexibly^{25,26}, without any air-feed antennas. The receiving horns 1 and 2 were fixed ~ 7.0 m away from the metasurface sample to receive the reflected BFSK signals 1 and 2, respectively. Due to the property of the FDM scheme, the interference between the two nearby receiving horn antennas can be well eliminated.

Workflow of the hybrid communication system

The light-to-microwave hybrid communication is performed in three stages. Firstly, each pixel of videos 1 and 2 is represented by a 32-bit binary sequence, and thus the

two videos can be converted into two sets of bit streams (such as '01010...' and '10010...'). The two sets of bit streams stored in FPGA are read bit by bit at the same time, combining into a set of 2-bit binary digits. The four states of the 2-bit binary digits are translated into different control signals through the FPGA and DAC modules for driving the light source to produce the corresponding light waveforms. Fig. S4a schematically shows the above mapping process. Secondly, when receiving the light signal, the metasurface platform will generate four sets of spectral distributions for implementing the dual-channel BFSK modulations under two subcarriers incidences. Finally, the two reflected BFSK signals are received by the RF receiver for processing. For BFSK demodulations, the time domain signal is first transformed into the frequency domain by using fast Fourier transform. Then in each channel the two frequency components of the fundamental frequency (f_L) and blue-shifted frequency (f_R) are compared with each other. If the power of the fundamental frequency is larger than that of the blue-shifted frequency, the received digital symbol is determined to be '0'; on the contrary, the received digital symbol is determined to be '1', as conceptually shown in Fig. S4b. It should be noted that from the measured spectral distributions in Fig. 3, we clearly see that the energy differences between the fundamental frequency and blue-shifted frequency are larger than 3 dB for all cases, which is large enough for the BFSK demodulations. After demodulation, two sets of bit streams are obtained and then the original videos are recovered using the post-processing programs. The complete workflow of the hybrid communication system is depicted in Fig. S4c.

Acknowledgements

This work was supported by the National Key Research and Development Program of China (2017YFA0700201, 2017YFA0700203, and 2016YFC0800401), the Major Project of the Natural Science Foundation of Jiangsu Province (BK20212002), the National Natural Science Foundation of China (61890544 and 61631007), the China National Postdoctoral Program for Innovative Talents (BX2021063), the China Postdoctoral Science Foundation (2021M700762), the Fundamental Research Funds for the Central Universities (2242021k30040), the Foundation of National Excellent Doctoral Dissertation of China (201444), and the 111 Project (111-2-05).

Author details

¹State Key Laboratory of Millimeter Waves, School of Information Science and Engineering, Southeast University, 210096 Nanjing, China. ²National Mobile Communications Research Laboratory, School of Information Science and Engineering, Southeast University, 210096 Nanjing, China. ³Frontiers Science Center for Mobile Information Communication and Security, Southeast University, 210096 Nanjing, China. ⁴Purple Mountain Laboratories, 211111 Nanjing, China. ⁵Department of Electrical and Computer Engineering, National University of Singapore, Singapore 117583, Singapore

Author contributions

W.X.J., T.J.C., and Z.Z. proposed the research direction, supervised the project, and contributed to the general concept and interpretation of the results. X.G.Z. conceived the idea, designed the research, and performed the experiments, in coordination with Y.L.S. and B.Z. X.G.Z. carried out the theoretical analysis and developed the metasurface. B.Z. and Y.L.S. designed and built the optical

transmitter. Y.L.S. and X.G.Z. designed and constructed the microwave receiver. X.G.Z. and Y.L.S. conducted the communication system measurements with the help of Q.Y., C.W.Q., and H.W.T. X.G.Z., Y.L.S., and B.Z. collected and analyzed the data. X.G.Z., Y.L.S., W.X.J., and T.J.C. co-wrote the manuscript with input and comments from all the authors.

Data availability

The data that support the plots within this paper and other findings of this study are available from the corresponding author upon reasonable request.

Conflict of interest

The authors declare no competing interests.

Supplementary information The online version contains supplementary material available at <https://doi.org/10.1038/s41377-022-00817-5>.

Received: 3 February 2022 Revised: 24 April 2022 Accepted: 25 April 2022

Published online: 06 May 2022

References

- Salamin, Y. et al. Direct conversion of free space millimeter waves to optical domain by plasmonic modulator antenna. *Nano Lett.* **15**, 8342–8346 (2015).
- Salamin, Y. et al. Microwave plasmonic mixer in a transparent fibre-wireless link. *Nat. Photonics* **12**, 749–753 (2018).
- Ummethala, S. et al. THz-to-optical conversion in wireless communications using an ultra-broadband plasmonic modulator. *Nat. Photonics* **13**, 519–524 (2019).
- Wijayanto, Y. N., Murata, H. & Okamura, Y. Electrooptic millimeter-wave–lightwave signal converters suspended to gap-embedded patch antennas on low- k dielectric materials. *IEEE J. Sel. Top. Quantum Electron.* **19**, 3400709 (2013).
- Ayata, M. et al. High-speed plasmonic modulator in a single metal layer. *Science* **358**, 630–632 (2017).
- Rahaim, M. et al. Welcome to the CROWD: design decisions for coexisting radio and optical wireless deployments. *IEEE Netw.* **33**, 174–182 (2019).
- Chowdhury, M. Z. et al. Optical wireless hybrid networks: trends, opportunities, challenges, and research directions. *IEEE Commun. Surv. Tutor.* **22**, 930–966 (2020).
- Harter, T. et al. Wireless THz link with optoelectronic transmitter and receiver. *Optica* **6**, 1063–1070 (2019).
- Stotts, L. B. et al. Hybrid optical RF airborne communications. *Proc. IEEE* **97**, 1109–1127 (2009).
- Bariah, L. et al. A prospective look: key enabling technologies, applications and open research topics in 6G networks. *IEEE Access* **8**, 174792–174820 (2020).
- Cui, T. J. et al. Coding metamaterials, digital metamaterials and programmable metamaterials. *Light: Sci. Appl.* **3**, e218 (2014).
- Tsilipakos, O. et al. Toward intelligent metasurfaces: the progress from globally tunable metasurfaces to software-defined metasurfaces with an embedded network of controllers. *Adv. Optical Mater.* **8**, 2000783 (2020).
- Zhang, X. G. et al. An optically driven digital metasurface for programming electromagnetic functions. *Nat. Electron.* **3**, 165–171 (2020).
- Zhang, X. G. et al. Light-controllable digital coding metasurfaces. *Adv. Sci.* **5**, 1801028 (2018).
- Zhang, X. G., Jiang, W. X. & Cui, T. J. Frequency-dependent transmission-type digital coding metasurface controlled by light intensity. *Appl. Phys. Lett.* **113**, 091601 (2018).
- Chen, M. K. et al. Principles, functions, and applications of optical meta-lens. *Adv. Optical Mater.* **9**, 2001414 (2021).
- Li, Z. P. et al. Metasurfaces for bioelectronics and healthcare. *Nat. Electron.* **4**, 382–391 (2021).
- Dorrah, A. H. et al. Metasurface optics for on-demand polarization transformations along the optical path. *Nat. Photonics* **15**, 287–296 (2021).
- Cui, T. J. et al. *Inf. Metamaterial Syst. iScience* **23**, 101403 (2020).
- Cui, T. J., Liu, S. & Zhang, L. Information metamaterials and metasurfaces. *J. Mater. Chem. C* **5**, 3644–3668 (2017).
- Cui, T. J. Microwave metamaterials. *Natl Sci. Rev.* **5**, 134–136 (2018).
- Ren, H. R. et al. Complex-amplitude metasurface-based orbital angular momentum holography in momentum space. *Nat. Nanotechnol.* **15**, 948–955 (2020).
- Zhang, X. G. et al. Polarization-controlled dual-programmable metasurfaces. *Adv. Sci.* **7**, 1903382 (2020).
- Chen, L. W., Li, Y. & Hong, M. H. Total reflection metasurface with pure modulated signal. *Adv. Optical Mater.* **7**, 1801130 (2019).
- Xu, P. et al. Phase and polarization modulations using radiation-type metasurfaces. *Adv. Optical Mater.* **9**, 2100159 (2021).
- Xu, P. et al. Radiation-type metasurfaces for advanced electromagnetic manipulation. *Adv. Funct. Mater.* **31**, 2100569 (2021).
- Shlezinger, N. et al. Dynamic metasurface antennas for 6G extreme massive MIMO communications. *IEEE Wirel. Commun.* **28**, 106–113 (2021).
- Dai, J. Y. et al. Wireless communication based on information metasurfaces. *IEEE Trans. Microw. Theory Tech.* **69**, 1493–1510 (2021).
- Tang, W. K. et al. Wireless communications with programmable metasurface: new paradigms, opportunities, and challenges on transceiver design. *IEEE Wirel. Commun.* **27**, 180–187 (2020).
- Di Renzo, M. et al. Smart radio environments empowered by reconfigurable intelligent surfaces: how it works, state of research, and the road ahead. *IEEE J. Sel. Areas Commun.* **38**, 2450–2525 (2020).
- Dai, L. L. et al. Reconfigurable intelligent surface-based wireless communications: antenna design, prototyping, and experimental results. *IEEE Access* **8**, 45913–45923 (2020).
- Cui, T. J. et al. Direct transmission of digital message via programmable coding metasurface. *Research* **2019**, 2584509 (2019).
- Wu, Q. Q. & Zhang, R. Towards smart and reconfigurable environment: intelligent reflecting surface aided wireless network. *IEEE Commun. Mag.* **58**, 106–112 (2020).
- Zhao, J. et al. Programmable time-domain digital-coding metasurface for non-linear harmonic manipulation and new wireless communication systems. *Nat Sci. Rev.* **6**, 231–238 (2019).
- Hodge, J. A., Mishra, K. V. & Zaghloul, A. I. Intelligent time-varying metasurface transceiver for index modulation in 6G wireless networks. *IEEE Antennas Wirel. Propag. Lett.* **19**, 1891–1895 (2020).
- Zhang, L. et al. A wireless communication scheme based on space- and frequency-division multiplexing using digital metasurfaces. *Nat. Electron.* **4**, 218–227 (2021).
- Shaltout, A. M., Shalae, V. M. & Brongersma, M. L. Spatiotemporal light control with active metasurfaces. *Science* **364**, eaat3100 (2019).
- Taravati, S. & Eleftheriades, G. V. Full-duplex nonreciprocal beam steering by time-modulated phase-gradient metasurfaces. *Phys. Rev. Appl.* **14**, 014027 (2020).
- Zhang, X. G. et al. Smart Doppler cloak operating in broad band and full polarizations. *Adv. Mater.* **33**, 2007966 (2021).
- Venkatesh, S. et al. A high-speed programmable and scalable terahertz holographic metasurface based on tiled CMOS chips. *Nat. Electron.* **3**, 785–793 (2020).
- Manjappa, M. et al. Reconfigurable MEMS Fano metasurfaces with multiple-input-output states for logic operations at terahertz frequencies. *Nat. Commun.* **9**, 4056 (2018).
- Li, X. et al. Multicolor 3D meta-holography by broadband plasmonic modulation. *Sci. Adv.* **2**, e1601102 (2016).
- Dou, K. et al. Off-axis multi-wavelength dispersion controlling metalens for multi-color imaging. *Opto-Electron. Adv.* **3**, 190005 (2020).
- Zhang, C. L., Zhang, D. F. & Bian, Z. P. Dynamic full-color digital holographic 3D display on single DMD. *Opto-Electron. Adv.* **4**, 200049 (2021).
- Liu, J. et al. Quantum photonics based on metasurfaces. *Opto-Electron. Adv.* **4**, 200092 (2021).
- Li, R. J. et al. Light-controlled metasurface with a controllable range of reflection phase modulation. *J. Phys. D: Appl. Phys.* **55**, 225302 (2022).
- da Costa, I. F. et al. Optically controlled reconfigurable antenna array for mm-wave applications. *IEEE Antennas Wirel. Propag. Lett.* **16**, 2142–2145 (2017).
- Tawk, Y. et al. Optically pumped frequency reconfigurable antenna design. *IEEE Antennas Wirel. Propag. Lett.* **9**, 280–283 (2010).
- You, X. H. et al. Towards 6G wireless communication networks: vision, enabling technologies, and new paradigm shifts. *Sci. China Inf. Sci.* **64**, 110301 (2021).
- Dang, S. P. et al. What should 6G be? *Nat. Electron.* **3**, 20–29 (2020).